A novel approach combining thermosiphon and phase change materials (PCM) for cold energy storage in cooling systems

Maria Aurely Yedmel, Romuald Hunlede, Stéphanie O.L. Lacour, Graciela Alvarez, Anthony Delahaye, Denis Leducq

A novel approach combining thermosiphon and phase change materials (PCMs) for cold energy storage in cooling systems

Maria Aurely Yedmel[a], Romuald Hunlede[a], Stéphanie Lacour[a], Graciela Alvarez[a], Anthony Delahaye [a], Denis Leducq *[a]

[a]Université Paris-Saclay, INRAE, FRISE, 92761 Antony, France

*Corresponding author: denis.leducq@inrae.fr

ABSTRACT

A novel approach combining thermal energy storage (TES) and a thermosiphon was investigated for cold storage. The use of TES units for cooling systems has been studied for many years, as they are well suited for short-term energy storage. A cold latent heat accumulator was designed to replace the function of any vapour compression cycle in the event of electrical failure without using any electrical device but rather the thermosiphon principle. A laboratory prototype of a thermosiphon combined with the cold accumulator was developed using a paraffin mixture as a phase change material (PCM). The accumulator was connected to the vapour compression system of a closed display cabinet. An experimental study was carried out by simulating 1.5-hour compressor shutdowns with and without the accumulator. The air and product temperatures in the cabinet, the behaviour of the compressor during restart, and the charging and discharging processes of the accumulator were analysed. The results showed that shutting down the compressor with the cold accumulator significantly reduces the increase of air and product temperatures compared to shutting down without the accumulator. The air temperature in the rear duct was maintained within the acceptable temperature range for 72 minutes with the accumulator, compared to 3 minutes without. A default in the design of the accumulator was observed during the charging phase, as some areas of

the accumulator never reached 80 % of charge. This new approach extends demand-side management and renewable energies to all end users of vapour compression machines.

Refrigeration, Cold storage, Thermosiphon, PCM, Power outages, Demand-side management

1. Introduction

Cooling systems are used to maintain or reduce the temperature of a fluid or a solid to a lower level. Typically, a refrigerant circulates through a vapour compression cycle where it removes heat from the cold source and transfers it to the hot source. Vapour compression systems are used for refrigeration (domestic, commercial, industrial, and transport refrigeration) and air conditioning (room and mobile air conditioning) (Dong et al., 2021) and are very energy intensive. Dupont et al. (2019) state that the refrigeration sector accounts for about 20 % of global electricity consumption. In 2018, 20 % of this share was attributable to electric fans and air conditioners installed in buildings (IEA, 2018). In addition, in industrialised countries, 30-60 % of the electricity consumed by supermarkets is due to refrigeration systems (UNIDO, 2020). In the context of global warming, several measures have been implemented to reduce the electricity consumption of vapour compression systems. One of these methods is to use thermal energy storage (TES) technologies to store thermochemical, latent, or sensible heat for later use and facilitate the use of intermittent renewable energy sources.

In the case of latent heat storage, phase change materials (PCMs) are used as the medium. PCMs can store heat or cold by changing phase, for example, from liquid to solid, and release this energy by changing phase as well, but in reverse, from solid to liquid. Phase change occurs at a temperature called the phase change temperature ($\mathrm{T_{pc}}$), which depends on the operating pressure and predefines the application of the PCM. PCMs can be organic compounds (paraffin/non-paraffin), inorganic compounds (salt hydrate/metal), or eutectic compounds (organic-organic, inorganic-inorganic, and organic-inorganic). Some benefits of organic PCMs are their chemical inertia, recyclability, low vapour pressure in the melt form, and small volume change during phase transition. Their low thermal conductivity and incompatibility with plastic containers are some disadvantages. Inorganic PCMs and mostly salt hydrates can be preferred for their availability, non-flammability, high latent heat of fusion, and high thermal conductivity. However, they are corrosive, irritant, and have high vapour pressure.(Memon, 2014)

PCMs can be added to building materials to reduce indoor temperature fluctuations and thus the energy consumption of air conditioning systems without increasing the structure' mass (Socaciu et al., 2014) (Memon, 2014). Hawes et al. (1989) studied the use of PCMS in concrete to store latent heat and found that among three different PCMs, DODECANOL ($\mathrm{T_{pc}}$: 21 °C) was the one that was compatible with both autoclaved concrete blocks and ordinary concrete blocks. Wang et al. (2022) successfully combined wild daisy flower stems with paraffin to obtain a stable composite ($\mathrm{T_{pc}}$: 40.1 °C) capable of regulating the temperature of a building by acting as a thermal buffer. In the refrigeration domain, PCMs can help to maintain product temperature and replace the cold machine during a given period. They are, therefore, massively studied in the literature to be used in insulated boxes, refrigerated trucks, domestic refrigerators, display cabinets, and cold storage facilities (Leungtongkum et al., 2022). In these studies, the PCM configuration (PCM melting point, quantity, position…) and the operating conditions (refrigerant temperature, ambient temperature, insulation material…) are crucial parameters. Ahmed et al. (2010) examined the effects of incorporating paraffin ($\mathrm{T_{pc}}$: 5 °C) into the insulation system of a refrigerated truck and observed that it reduced heat transfer and temperature fluctuations by 16.3 %. Liu et al. (2012) proposed a new refrigeration system with inorganic salt ($\mathrm{T_{pc}}$: -30.6 °C) inside the refrigerated truck and the refrigeration unit placed outside. The new system reduced energy costs by 50 % and maintained the truck's temperature at -18 °C for 10 hours in extreme weather conditions ($\mathrm{T_{pc}}$: 41 °C). Oró et al. (2012) studied the integration of Climsel ($\mathrm{T_{pc}}$: -18 °C) in a vertical freezer and found that during a 3-hour power failure, the air and product temperature increased less with the PCM than without (6 °C less and 2 °C less, respectively). Azzouz et al. (2009) placed water (T_{pc}: 0 °C) on the back of the evaporator of a domestic refrigerator, increasing its coefficient of performance (COP) by 10-30 % and allowing continuous operation for 5-6 hours without electricity. Additionally, Maiorino et al. (2019) utilised water as PCM placed on top and bottom of refrigerator shelves. Compared to a 3.1 °C temperature difference between two shelves without PCM, 0.2 °C was observed with PCM.

About display cabinets, fewer works were reported in the literature. Alzuwaid et al. (2015) placed heat exchanger with water gel (T_{pc}: -2 °C) in the rear channelling of an open-door refrigerated display cabinet. Temperatures in the products were homogenised, the compressor running time was decreased, and the maximum air temperature was reduced by 2 °C. Water (T_{pc}: 0 °C) was also integrated into an open-door display cabinet (Ben-Abdallah et al., 2019). During 2 hours of compressor downtime, products temperature increased by 1 °C, with the PCM heat exchanger, compared to 2 °C without the PCM heat exchanger. However, adding the heat exchanger without PCM in the rear duct decreased the air velocities at the discharge air grid (-28 % air curtain flowrate) and the fifth shelf. This decrease in air velocity results in higher product temperatures at the front and fifth shelves than without the heat exchanger (for example, from 4.4 °C without the heat exchanger to 7.9 °C with the heat exchanger). Ben-Abdallah et al. (2019) confirmed that the position of the PCM in the refrigerated display cabinet is essential to avoid any unwanted melting or obstruction of the cold air passage.

Thermosiphon technology shows high potential to fully utilise PCM potential without obstructing airflow since the proximity between the PCM and the evaporator is not required anymore. Thermosiphon effect is driven by the natural circulation of fluids due to the difference in density. It requires no electrical or mechanical components to move the fluid, thus saving energy. Many researchers have recently proposed to optimise cooling systems using thermosiphon technology. Lee et al. (2009) designed a hybrid cooler capable of operating in both vapour compression and thermosiphon modes depending on the ambient temperature. In the nuclear sector, the thermosiphon loop is considered as an efficient and reliable long-term cooling system for the spent fuel pool (Ye et al., 2013) (Fu et al., 2015) (Trewin, 2021). Li et al. (2018) investigated a two-phase thermosiphon loop to cool a motorised spindle shaft and observed improved heat transfer performance. Sutanto et al. (2022) integrated thermosiphon in a floating photovoltaic (PV) system and noted an increase of 7.86 % in the panels' power output compared to ground PV and an increase of 3.34 % compared to floating PV without thermosiphon.

For refrigeration systems, two-phase loop thermosiphons were studied to characterise the fluid flow and to understand the effects of operating parameters on its performance (Zhang et al., 2015) (Albertsen and Schmitz, 2021) (Wang et al., 2023). Coupled with PCM, thermosiphon can be used as a new energy-efficient optimisation technology for cooling systems. FOSTER et al. (2013) and Foster et al. (2015) compared the use of electricity to the use of a thermosiphon coupled with PCM for display cabinet defrosting. The thermosiphon melted the frost faster than the electric defrosting and reduced the total energy consumption of the cabinet. Liu et al. (2021) investigated the capacity of a two-phase loop thermosiphon to accurately regulate the temperature of the fresh food compartment of a modified refrigerator. The loop was coupled to a PCM (mixture of NaCl, $C_3H_8O_3$, and H_2O), located in the freezer, to provide cooling to the fresh food section. The system was successful in regulating the temperature of the compartment.

This paper aims to present the working principle of a novel thermal energy storage device combining PCM and thermosiphon technologies. The accumulator is designed to replace the cooling machine during voluntary or involuntary power outages in order to reduce energy consumption and enhance the implementation of renewable energy and demand-side management. The originality of the accumulator lies in the fact that it can be plugged into any current vapour compression cycle without the need for a secondary fluid or an atypical/additional cooling system and without obstructing the airflow or any other part of the existing system. The characteristics of the accumulator and its functioning when inserted into the vapour compression cycle of the equipment are detailed in the paper. The accumulator was tested in a closed-door instrumented refrigerated display cabinet. The changes in air and product temperatures during a 2-hour demand side management (compressor shutdown) with and without the accumulator are presented.

2. Material and methods

2.1 Accumulator description and integration in a vapour compression cycle

2.1.1 Cold storage accumulator design

A vapour compression machine has four main components: an expansion valve, an evaporator, a compressor, and a condenser. As the refrigerant passes through the loop, it undergoes multiple compression and expansion cycles, producing continuous cooling by absorbing heat from the evaporator and rejecting it to the surrounding environment through the condenser. Thermal energy storage can be achieved either by convective exchange with cold air, by direct contact of the material with the evaporator, or by using a secondary fluid. Placing the PCM in the cold air stream produced at the evaporator encroaches on the volume dedicated to storage, thus limiting the amount of PCM or product stored. When applied in contact with the evaporator, the PCM can also impinge on airflow (Ben-Abdallah et al., 2019) and reduce the exchange surface of the evaporator, thus decreasing its performance. Besides, there is no control over the charge and discharge periods of the PCM due to compressor shutdown cycles. The most common method is to use a secondary refrigerant to transport the cold from the evaporator to a remote storage unit and return it when needed. However, this involves two levels of heat exchange, which reduce the thermodynamic efficiency of the system and increase energy consumption and cost.

The novel system controls charging and discharging phases without a secondary refrigerant and therefore has better thermodynamic efficiency. The PCM is placed in a container with a finned tube heat exchanger, and this unit (accumulator) is well insulated with foam rubber to limit heat exchange with the surrounding environment. During the charging phase, thermal energy is stored in the accumulator while the refrigerating machine is running by direct exchange between the PCM and the refrigerant circulating in the copper tubes. The charging phase must be fast so that the accumulator can be charged at any time and the cooling machine can be replaced in case of need. The aluminium fins of the heat exchanger increase the exchange surface between the PCM and the refrigerant, which increases the efficiency of heat transfer. During the discharging phase (in the absence of electricity), the cold is returned to the evaporator by the thermosiphon effect. This stored cold energy must be able to meet the thermal load requirements at the evaporator. For this, the properties of the chosen PCM are crucial in determining the required volume of the accumulator and thus the amount of energy available during discharging phase. This charging and discharging principle is independent of the evaporator technology used by the machine. An additional system for a second refrigerant loop is not required, which reduces the cost. The accumulator can be placed outside the cold chamber, and thus does not occupy the space foreseen for the refrigerated products.

2.1.2 Cold storage accumulator integration and thermosiphon loop

Figure 1 shows the insertion of the accumulator in the vapour compression cycle. The accumulator is connected to the loop at the evaporator inlet. A set of controllable valves (V1-V4) is used to control the charge and discharge of the accumulator. The cooling circuit also includes a thermostatic expansion valve (TXV) to maintain a satisfactory refrigerant level in the evaporator. Valves 1 and 3 are closed during the charging phase; while valves 2 and 4 are open (Figure 1.a). The refrigerant leaves the thermostatic expansion valve and enters the accumulator, where it transfers cold energy to the PCM. The PCM drops in temperature and solidifies, while the refrigerant partially evaporates. The refrigerant then finishes exchanging thermal energy when it passes through the evaporator and leaves it as vapour. Therefore, when the PCM is completely solid, all the energy carried by the refrigerant is transferred to the evaporator.

In the discharging phase (power cuts), valves 1, 2, and 4 are closed while valve 3 is open, creating a closed circuit between the evaporator and the accumulator (Figure 1.b). In the evaporator, the liquid refrigerant absorbs heat from the element to be cooled (through heat exchange with air) and then evaporates. As a result of the pressure difference between the evaporator and the accumulator (in the vertical duct), a refrigerant flow due to thermosiphon effect takes place, and the vapour rises towards the accumulator. The refrigerant in vapour form condenses by absorbing the cold energy previously stored in the PCM. The refrigerant in liquid form flows back to the evaporator due to gravity forces, and the cycle is repeated. The PCM gradually heats up until it becomes totally liquid. At that point, there is no longer enough energy in the PCM to cool down the refrigerant to its liquid form. The refrigerant stays in its vapour state and is no longer recirculated.

The thermosiphon allows the system to operate at around 7 % of the power consumption when the compressor is on. The evaporator fan is still functioning to enable heat transfer between the refrigerant and air. Charging and discharging efficiencies are influenced by the height difference between the accumulator and the evaporator, since gravity is the driving force. An increase in height difference therefore leads to an increase in thermosiphon performance. However, after a critical height, the increase in vapour pressure drop can reduce its performance (Lee et al., 2009).

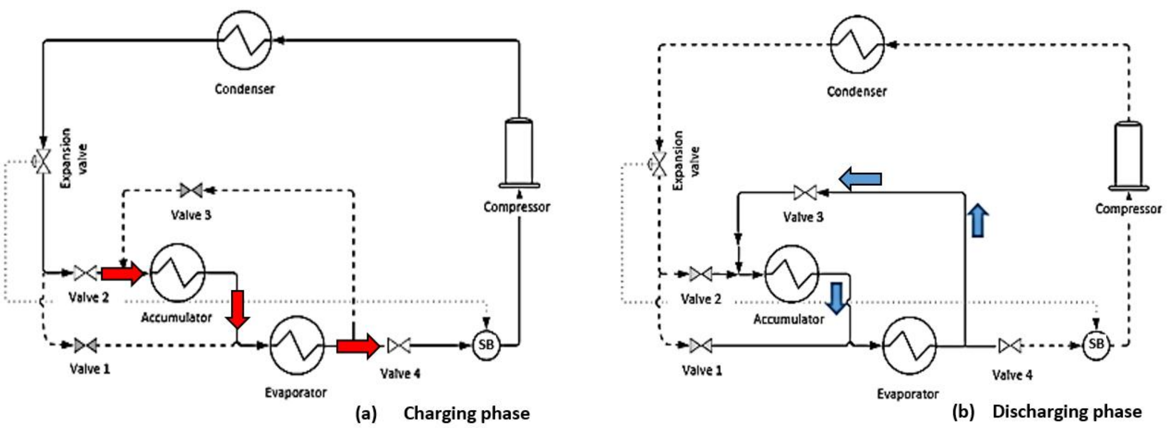

Figure 1. Diagram of the cold storage accumulator integrated into a vapour compression cycle during charging phase (a) and discharging phase (b)

2.2 Experimental setup and methods

2.2.1 Integration of the accumulator in a display cabinet

The accumulator (92 x 11 x 26 cm) was integrated into the original vapour compression system of a commercial closed vertical refrigerated display cabinet (OFFLIP 2 Eco DV; 200 x 134.5 x 70.5 cm). The accumulator was located outside the cabinet, in the upper rear part. The height of the riser (OD: 12.7 mm; ID: 10.9 mm) and downcomer (OD: 12.7 mm; ID: 10.9 mm) is 152 cm and 125 cm respectively. The display cabinet was a ventilated plug-in cabinet with positive cold storage (0/+2 °C). The PCM used is a chemically inert liquid paraffin mixture (RUBITHERM RT-4) with a phase change temperature T_{pc} from -4 °C to -7 °C, a liquid density of 0.76 kg/l at 15 °C and a storage capacity of 180 kJ/kg ± 7.5 %. About 20 kg of PCM was used for the experiment.

2.2.2 Display cabinet and accumulator instrumentation

The display cabinet and the accumulator were equipped with calibrated T-type thermocouples (uncertainty of ± 0.1 °C) (Figure 2). The air temperature was monitored in the rear duct, on the shelves, at the discharge air grid, and at the air curtain using 14 sensors. The display cabinet was loaded with methylcellulose packages (20 × 10 × 5 cm) to simulate food products. About 90 % of the storage volume was occupied in order to simulate a fully loaded display cabinet. The first 4 shelves had 3 columns of products in depth, and the fifth shelf had 4 columns. All the shelves had 6 rows of products of different heights in width. The temperature of the products (core and surface) was measured using 8 sensors. A total of 5 sensors were used to measure the temperature of the PCM in the accumulator. Two additional sensors measured the temperature of the refrigerant at the inlet and outlet of the accumulator. The compressor and condenser of the refrigeration system were also instrumented to evaluate the energy consumption of the display cabinet. Two temperature sensors were placed at the compressor inlet and outlet, and one was used at the condenser outlet. Two pressure sensors were also placed at the compressor inlet and outlet. A Wattmeter was used to measure the power consumed by the cabinet: compressor, fan, and lighting. The tests were carried out in a temperature-controlled room, and the room temperature was monitored. The measurements were recorded using a data acquisition system (Agilent 34970A) at an interval of 10 s after the start of the tests.

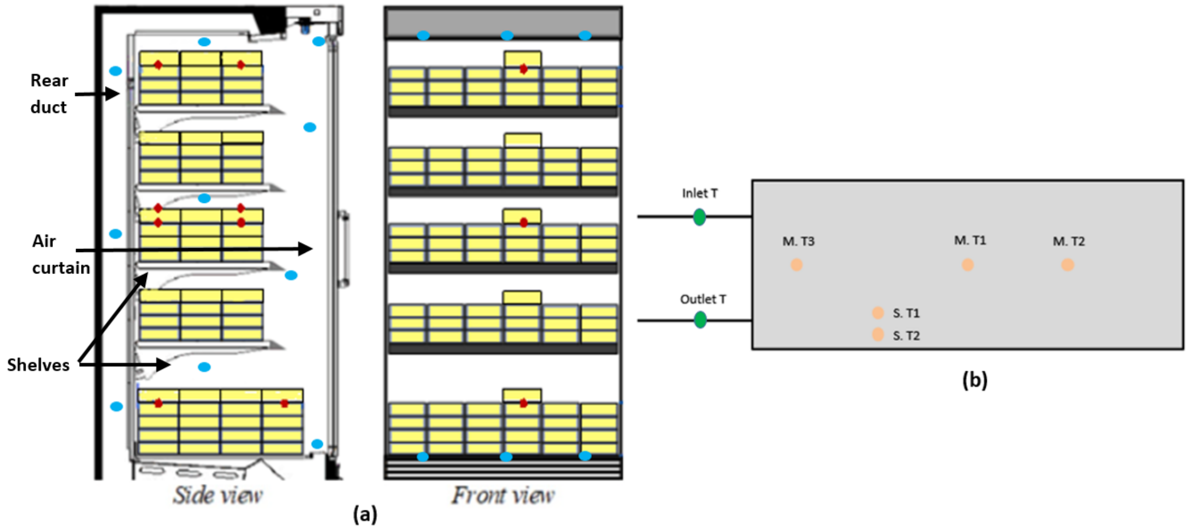

Figure 2. Illustration of thermocouple arrangement for temperature measurements of air and product (a); PCM and refrigerant (b)

2.2.3 Test protocol

The test was conducted in a temperature-controlled chamber at 17 °C (± 0.7 °C). The temperature of the cabinet thermostat was set to -3 °C and the doors remained closed for the experiment. Before starting the experiment, the closed display cabinet was run for 24 hours in charging mode to ensure that the PCM was fully charged and that the system reached a steady state.

When the systems reached stability, the compressor was shut down twice for 1.5 hours to check the ability of the accumulator to replace the refrigeration system using the thermosiphon principle. During the first shutdown, the system was put into discharging mode using the control valves. Thus, the accumulator was able to supply cold to the display cabinet. For comparison purposes, during the second shutdown, the system was operated without the accumulator by closing valves 2 and 3 (Figure 1).

3. Results and discussion

3.1 Accumulator charging and discharging processes

The charging rate of the accumulator was determined by using the enthalpy versus temperature curve. It allows the determination the amount of energy absorbed from the temperature of the PCM. The 5 thermocouples (3 middle thermocouples and 2-sided thermocouples) placed in the accumulator allow to know the state (solid or liquid) of each designated portion of PCM and thus the state of charge of each portion. The overall charging rate of the accumulator is estimated by taking the arithmetic average of the charging rate of each area. Figure 3 shows the evolution of the temperature of the PCM in the accumulator and Figure 4 presents the evolution of the accumulator charging rate per area during the first shutdown (discharging).

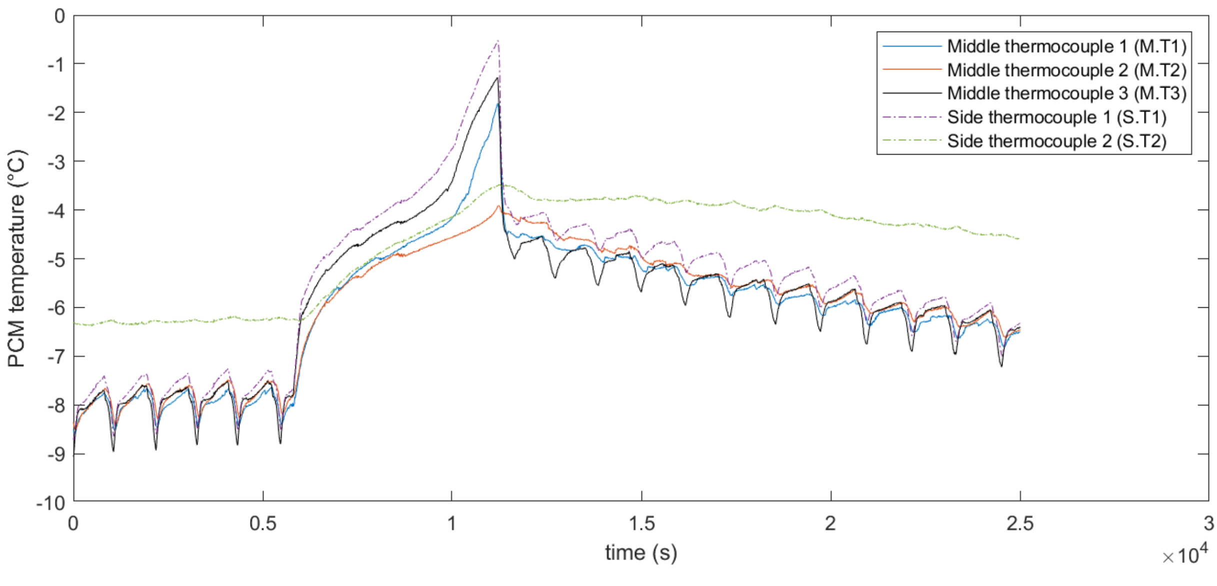

Figure 3. PCM temperature in different areas of the accumulator during the first shutdown (discharging)

As shown in Figure 3, the accumulator was fully charged at the beginning of the first shutdown except for the edges where the temperature was above -7 °C. The temperature at the edges of the accumulator is given by the two lateral thermocouples (S.T1) and (S.T2). This gap in the charging rate is due to the current configuration and dimensions of the accumulator. The heat transfer is maximum in the centre due to the circulation of the refrigerant in the heat exchanger tubes. Moreover, the size of the fins does not allow an optimal transfer to the edges of the accumulator, resulting in a slow charging rate of this area (data given by S.T2). During the compressor shutdown, the temperature of the PCM rises because of the heat exchange between the refrigerant and the PCM (Figure 3). When the thermosiphon effect is activated, the heat absorbed by the refrigerant from the products is released into the accumulator. The accumulator then gradually discharges, transferring the previously stored thermal energy (during the charging phase) to the refrigerant (Figure 4). This heat transfer is shown in Figure 5.

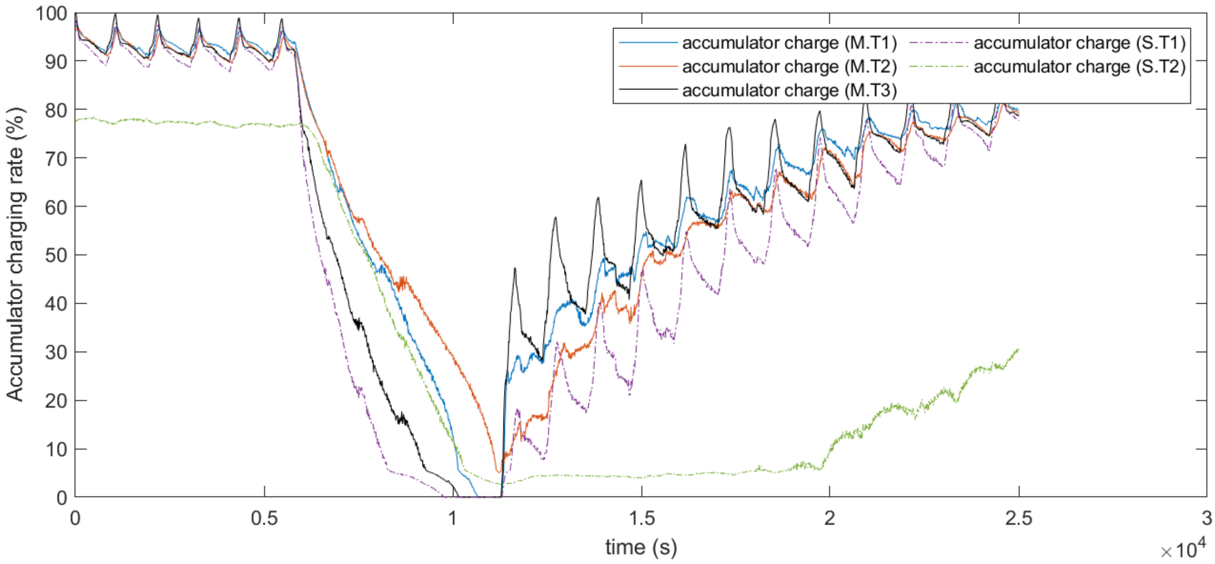

Figure 4. Evolution of the charging rate of the accumulator per area during the first shutdown

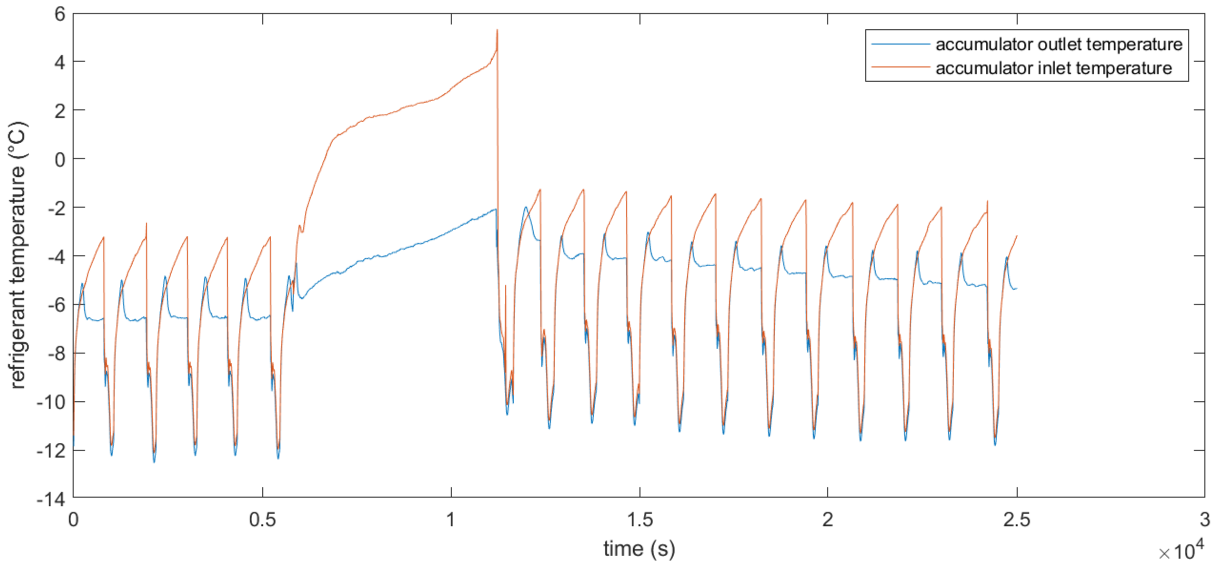

Figure 5. Evolution of the refrigerant inlet and outlet temperatures at the accumulator during the first shutdown

Before the compressor shutdown, the inlet and outlet temperatures of the refrigerant were approximately -5 °C (± 2.43 °C) and -6 °C (± 1.91 °C) respectively. At that time, the accumulator was fully charged and therefore there was little/no heat transfer between the refrigerant and the PCM. During the compressor shutdown, the temperature of the refrigerant entering the accumulator started to rise due to the absorption of heat from the cabinet products. The accumulator successfully lowers the refrigerant temperature from about 2 °C (± 1.42 °C) to about -4 °C (± 0.81 °C), which is quite close to the refrigerant outlet temperature when the compressor is operating (-6 °C ± 1.91 °C). After the compressor is restarted, it takes, on average, 98 minutes to charge the accumulator from 3 % to 50 %. The accumulator takes longer to charge than to discharge because, during the charging phase, the cold transported by the refrigerant is shared between the accumulator and the display cabinet, whereas during the discharging phase, the refrigerant uses the cold stored in the accumulator to satisfy the needs of the entire cabinet.

3.2 Air and products temperature evolution

Figure 6 illustrates the evolution of the cabinet's air temperature during the two compressor shutdowns in the rear duct, in the shelves and air curtain.

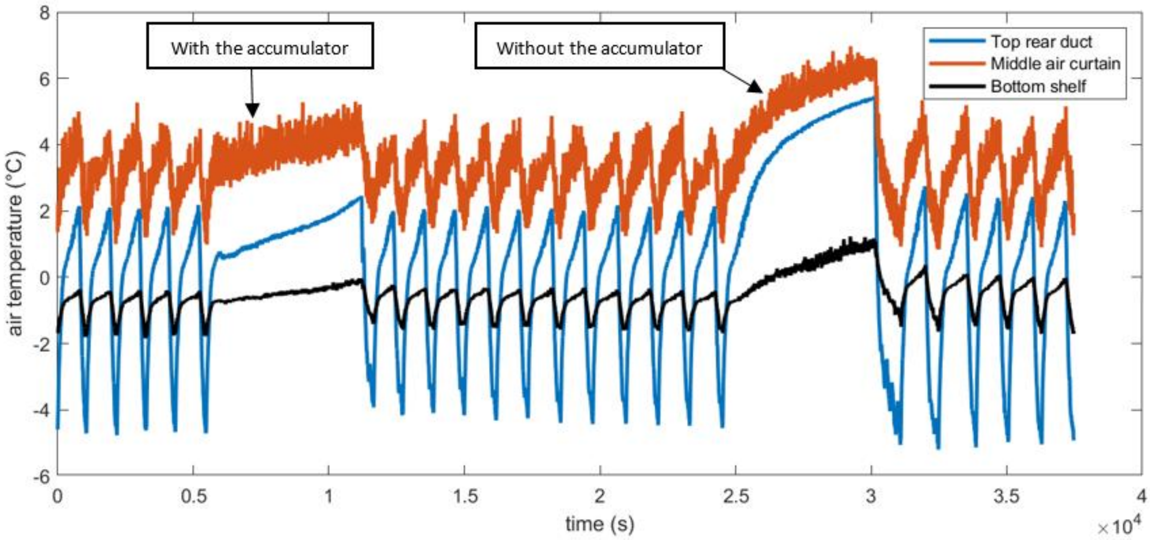

Figure 6. Evolution of the cabinet's air temperature during the two compressor shutdowns

During normal operation (between the two shutdowns), the air temperature varies because of the compressor's on/off cycles. These variations are always less than 2.2 °C for the air temperature in the rear duct, 2.3 °C for the air temperature in the shelves and 4.9 °C for the air temperature in the air curtain. The significant disturbances observed for the air curtain temperature are due to the influence of the ambient temperature, as the cabinet doors are not hermetically closed. The air temperature rises more slowly during the first shutdown (with accumulator) than during the second one (without the accumulator). In fact, during the first shutdown, the accumulator successfully manages to keep the air temperature within the acceptable temperature range (normal operation) for 72 minutes in the rear duct and 48 minutes in the shelves and the air curtain. However, during the second shutdown (without the accumulator), it only takes 3 minutes, 5 minutes and 7 minutes, respectively, for the air temperature to exceed the permissible temperature range in the rear duct, in the shelves and in the air curtain. The air temperature rises rapidly without the accumulator because no cooling is provided to the cabinet, which leads to heat build-up. The slow increase in the air temperature with the accumulator is because cooling is provided to the cabinet due to the accumulator discharging its cold energy through the thermosiphon effect. Figure 7 presents the increase in air temperature (histogram) and the maximum air temperature reached (line) in the rear duct, shelves and air curtain during the two compressor shutdowns and normal operation. The increase in air temperature was evaluated based on a reference temperature corresponding to the lowest temperature reached in normal operation for each position. The maximum increase in air temperature during normal operation is 6.2 °C compared with 7.1 °C when the compressor is shut down with the accumulator and 10.3 °C when the compressor is shut down without the accumulator. In the current configuration, for all positions, the accumulator slows the increase in air temperature but cannot stabilise it due to a lack of cooling power delivered towards the end of the shutdown time. However, it enables the cabinet to perform closer to normal operation. It is essential to note that the thermal inertia provided by the cabinet products also dampens the air temperature increase. If the percentage of the cabinet's storage volume occupied by the products were less than 90 %, the increase would have been more significant for both cases (with and without accumulator).

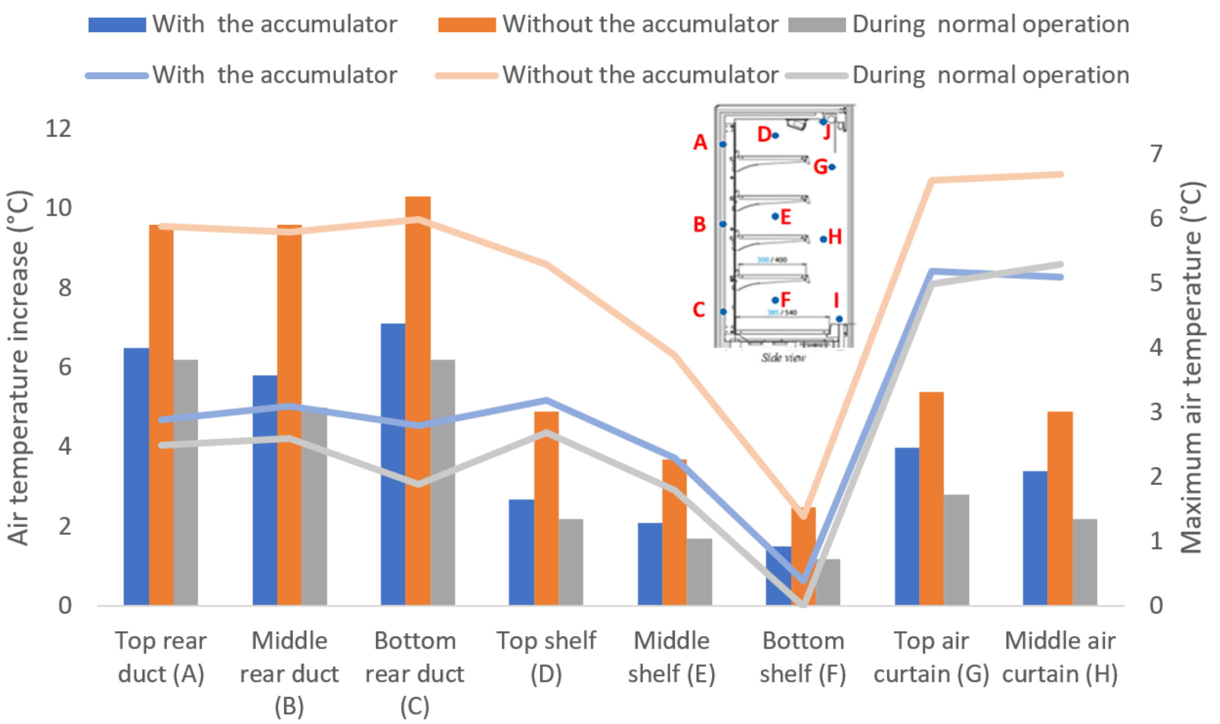

Figure 7. Air temperature increase (histogram) and maximum air temperature (line) in the cabinet during the compressor shutdowns and normal operation

The temperature evolution of the products during the two shutdowns is presented in Figure 8. The temperature variation between the shutdowns is due to the compressor on/off cycles during normal operation.

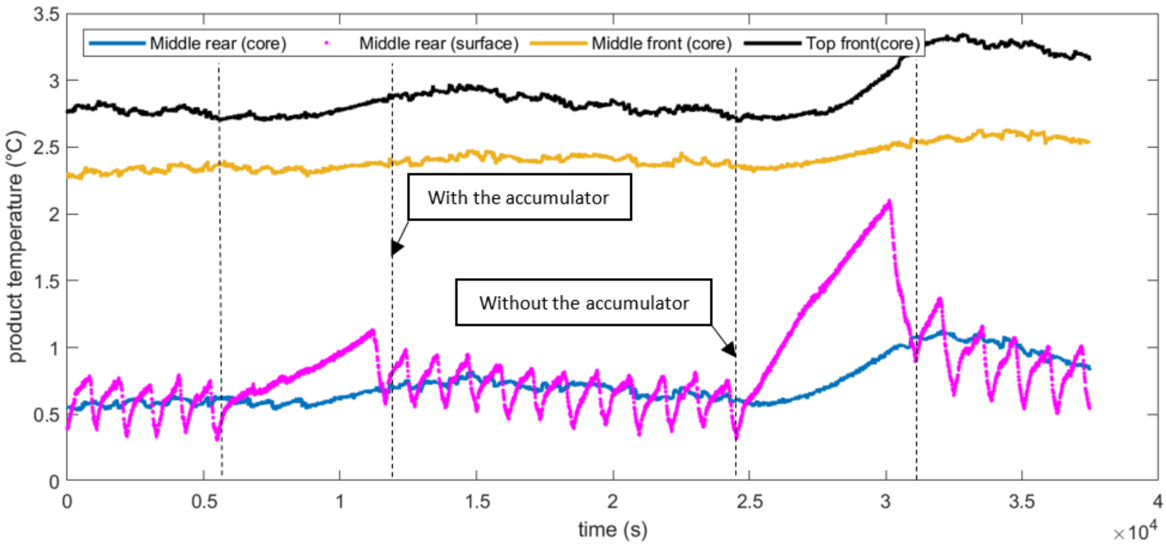

Figure 8. Evolution of the product temperature in the cabinet during the two compressor shutdowns

As expected, the temperature of the products rises more slowly during the shutdown with the accumulator than without the accumulator. The temperature of the products is affected differently depending on the products' position in the cabinet. The two compressor shutdowns had logically less impact on the products' core temperature than on the products' surface temperature, as shown by the different slopes, due to the thermal inertia acquired by the products during normal operation and because the surface of the products is the first part to be in contact with the (warmer) air. Products located at the rear are colder than products located at the front during normal operation and during the two shutdowns, as they are closest to the air distribution channels. Figure 9 presents the temperature rise (histogram) and maximum temperature reached (line) by the products depending on their position within the cabinet during compressor shutdowns and normal operation.

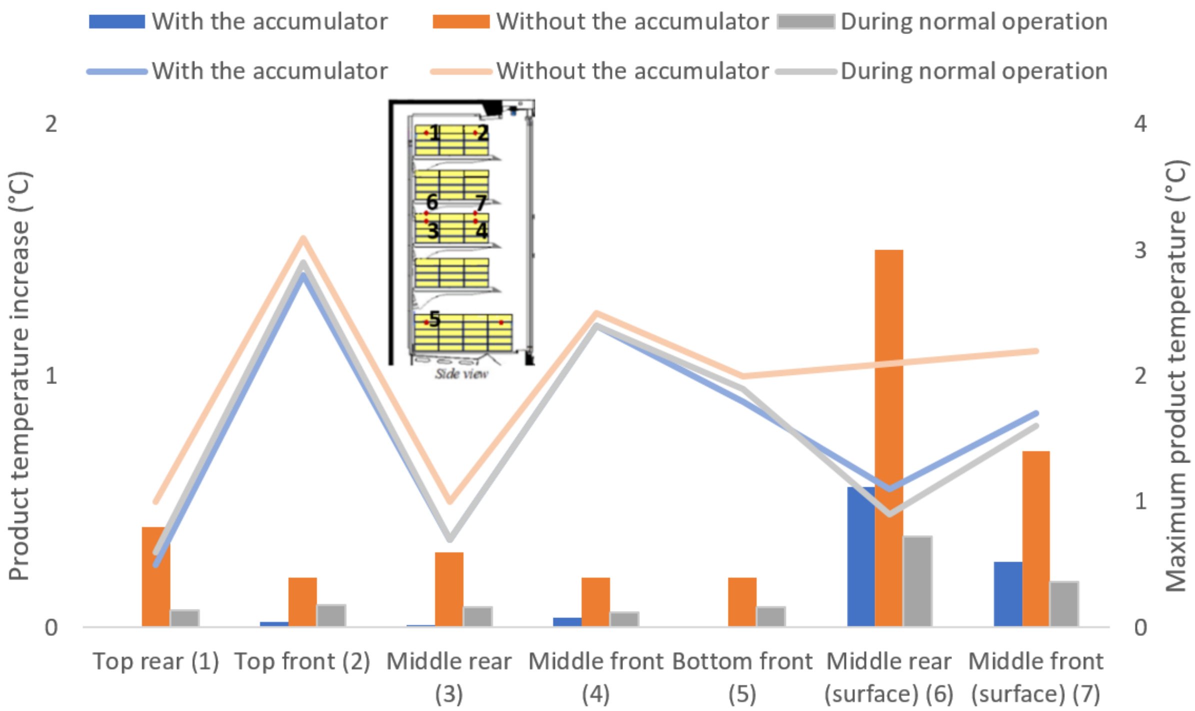

Figure 9. Increase in temperature (histogram) and maximum temperature (line) reached by the products depending on their position in the cabinet during compressor shutdowns and normal operation

Discharging the accumulator during the first shutdown kept the core temperature of the products below the maximum temperature reached during normal operation. All increases in product temperatures were less than 0.6 °C. During the second shutdown (without the accumulator), the product temperatures were maintained below the acceptable temperature for longer than the air temperatures, thanks to the thermal inertia of the products. The longest holding time was 71 minutes (for the bottom products). The maximum increase observed in the case of the shutdown without the accumulator was 1.5 °C. As the core of the products reacts slowly to air temperature changes in the cabinet, after each shutdown (with and without the accumulator), when the compressor has been restarted, the core temperature of the products continues to rise for a period that depends on the position of the products in the cabinet, before decreasing. The cabinet's temperature at the end of each shutdown affects the behaviour of the compressor when it is switched on again.

3.3 Compressor behaviour

Figure 10 presents the pressure at the compressor inlet and outlet during the two shutdowns. The on/off cycles responsible for the temperature variations in the accumulator, air and products during normal operation are also illustrated.

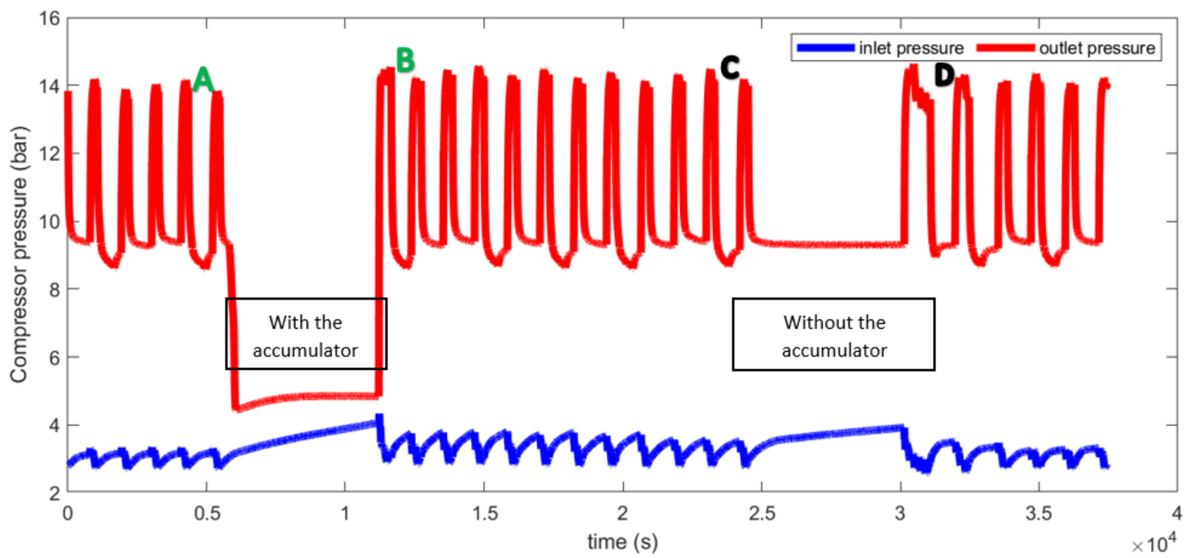

Figure 10. Evolution of the compressor's inlet and outlet pressure during the two shutdowns

During the shutdown with the accumulator, the compressor outlet pressure falls to the same level as the inlet pressure due to the activation of the thermosiphon loop. In fact, in order to trap a sufficient amount of refrigerant in the loop, when the compressor is shut down, the sensing bulb of the thermostatic expansion valve (TXV) (Figure 1) triggers the opening of the TXV by heating up, which considerably reduces the pressure in the compressor outlet channel. During the shutdown without the accumulator, the outlet pressure at the compressor is the same as for a defrost period or an off cycle because the TXV opening is not forced. When the compressor is restarted, the running time of the compressor is longer after shutdown without the accumulator (about 931 s) than after shutdown with the accumulator (about 430 s) (Figure 11). In the case of the shutdown without the accumulator, the compressor runs longer to compensate for the high-temperature increase in the cabinet (and therefore consumes more energy). In contrast, in the case of the shutdown with the accumulator, the compressor runs less because the accumulator was able to reduce the temperature rise in the cabinet during the shutdown (and therefore consumes less energy).

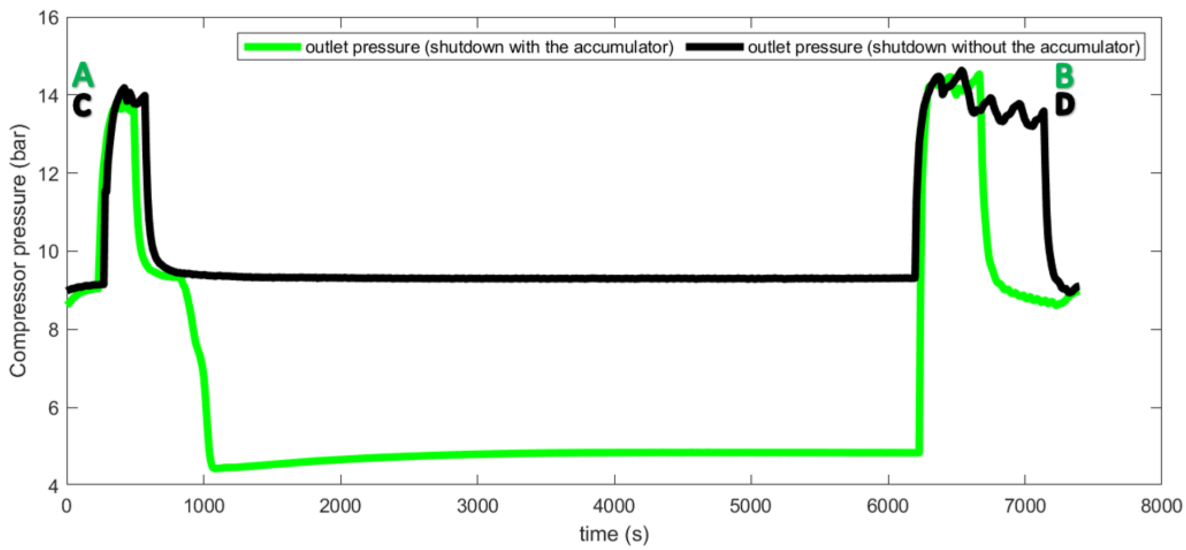

Figure 11. Evolution of the compressor's outlet pressure during the two shutdowns

4. Conclusion

This paper presents the working principle of a novel thermosiphon accumulator for cold storage applications. The accumulator was designed to supply cold energy to the evaporator of any vapour compression cycle machine during power cuts. It combines a phase change material to store thermal energy and thermosiphon principle to release it. The ability of the accumulator to properly perform its function as a cold provider was tested experimentally on the vapour compression cycle of a closed refrigerated display cabinet. The compressor was shut down for 1.5 hours with and without the accumulator. The temperature in the display cabinet and the accumulator, as well as the behaviour of the compressor, were studied.

In summary, the heat transfer inside the accumulator is not homogeneous, and charging takes longer than discharging (22 minutes to discharge from 89 % to 50 % compared with 98 minutes to charge from 3 % to 50 %). Nevertheless, air and product temperatures rise slowly when the compressor is shut down with the accumulator. The maximum increase in air and products temperatures with the accumulator is 7.1 °C and 0.6 °C respectively, while without the accumulator, it is 10.3 °C and 1.5 °C respectively. The compressor runs longer after the shutdown without the accumulator to reduce the high-temperature rise in the cabinet. The accumulator can increase the lifespan of products in case of sudden compressor breakdown. As long as enough energy is stored in the PCM, the system can deliver it to the evaporator, thus promoting intermittent energies, demand side management, and increasing product safety.

In further work, the internal design of the accumulator and the impact of operating parameters (such as product loading, thermostat temperature, ambient temperature, and door opening) will be studied in more detail, as they are thought to have an impact on the accumulator charging process and the temperature rise in the cabinet, respectively. The energy consumption of the display cabinet with the accumulator will also be assessed and compared to the energy consumption without the accumulator.

REFERENCES

AHMED, M., MEADE, O. & MEDINA, M. A. 2010. Reducing heat transfer across the insulated walls of refrigerated truck trailers by the application of phase change materials. *Energy Conversion and Management,* 51**,** 383-392.

ALBERTSEN, B. & SCHMITZ, G. 2021. Experimental parameter studies on a two-phase loop thermosyphon cooling system with R1233zd(E) and R1224yd(Z). *International Journal of Refrigeration,* 131**,** 146-156.

ALZUWAID, F., GE, Y. T., TASSOU, S. A., RAEISI, A. & GOWREESUNKER, L. 2015. The novel use of phase change materials in a refrigerated display cabinet: An experimental investigation. *Applied Thermal Engineering,* 75**,** 770-778.

AZZOUZ, K., LEDUCQ, D. & GOBIN, D. 2009. Enhancing the performance of household refrigerators with latent heat storage: An experimental investigation. *International Journal of Refrigeration,* 32**,** 1634-1644.

BEN-ABDALLAH, R., LEDUCQ, D., HOANG, H. M., FOURNAISON, L., PATEAU, O., BALLOT-MIGUET, B. & DELAHAYE, A. 2019. Experimental investigation of the use of PCM in an open display cabinet for energy management purposes. *Energy Conversion and Management,* 198.

DONG, Y., COLEMAN, M. & MILLER, S. A. 2021. Greenhouse Gas Emissions from Air Conditioning and Refrigeration Service Expansion in Developing Countries. *Annual Review of Environment and Resources,* 46**,** 59-83.

DUPONT, J.-L., DOMANSKI, P., LEBRUN, P. & ZIEGLER, F. 2019. The role of refrigeration in the global economy - 38 Informatory Note on Refrigeration Technologies. France.

FOSTER, A., CAMPBELL, R., DAVIES, T. & EVANS, J. 2013. A novel pcm thermo siphon defrost system for a frozen retail display cabinet. *2nd IIR Conference on Sustainability and the Cold Chain.* Paris.

FOSTER, A., CAMPBELL, R., DAVIES, T. & EVANS, J. 2015. *A novel passive defrost system for a frozen retail display cabinet with a low evaporator. T.*

FU, W., LI, X., WU, X. & ZHANG, Z. 2015. Investigation of a long term passive cooling system using two-phase thermosyphon loops for the nuclear reactor spent fuel pool. *Annals of Nuclear Energy,* 85**,** 346-356.

HAWES, D. W., BANU, D. & FELDMAN, D. 1989. Latent heat storage in concrete. *Solar Energy Materials,* 19**,** 335-348.

IEA 2018. The Future of Cooling: Opportunities for energy-efficient air conditioning. Paris: IEA.

LEE, S., KANG, H. & KIM, Y. 2009. Performance optimization of a hybrid cooler combining vapor compression and natural circulation cycles. *International Journal of Refrigeration,* 32**,** 800-808.

LEUNGTONGKUM, T., FLICK, D., HOANG, H. M., STEVEN, D., DELAHAYE, A. & LAGUERRE, O. 2022. Insulated box and refrigerated equipment with PCM for food preservation: State of the art. *Journal of Food Engineering,* 317**,** 110874.

LI, F., GAO, J., SHI, X., LIANG, F., ZHU, K. & LI, Y. 2018. Experimental investigation of an R600a two-phase loop thermosiphon to cool a motorized spindle shaft. *International Communications in Heat and Mass Transfer,* 97**,** 9-16.

LIU, M., SAMAN, W. & BRUNO, F. 2012. Development of a novel refrigeration system for refrigerated trucks incorporating phase change material. *Applied Energy,* 92**,** 336-342.

LIU, W., CHEN, C., CAO, J., WU, L., REN, W., JIAO, D. & PEI, G. 2021. Experimental study of a novel cool-storage refrigerator with controllable two-phase loop thermosyphon. *International Journal of Refrigeration,* 129**,** 32-42.

MAIORINO, A., DEL DUCA, M. G., MOTA-BABILONI, A., GRECO, A. & APREA, C. 2019. The thermal performances of a refrigerator incorporating a phase change material. *International Journal of Refrigeration,* 100**,** 255-264.

MEMON, S. A. 2014. Phase change materials integrated in building walls: A state of the art review. *Renewable and Sustainable Energy Reviews,* 31**,** 870-906.

ORÓ, E., MIRÓ, L., FARID, M. M. & CABEZA, L. F. 2012. Improving thermal performance of freezers using phase change materials. *International Journal of Refrigeration,* 35, 984-991.

SOCACIU, L., PLESA, A., UNGURESAN, P. & GIURGIU, O. 2014. Review on phase change materials for building applications. *Leonardo Electronic Journal of Practices and Technologies,* 13, 179-194.

SUTANTO, B., INDARTONO, Y. S., WIJAYANTA, A. T. & IACOVIDES, H. 2022. Enhancing the performance of floating photovoltaic system by using thermosiphon cooling method: Numerical and experimental analyses. *International Journal of Thermal Sciences,* 180, 107727.

TREWIN, R. R. 2021. Development of a one-dimensional model of a closed thermosiphon for cooling a spent-fuel pool. *Nuclear Engineering and Design,* 374, 111027.

UNIDO 2020. Towards energy efficient retail refrigeration in developing countries. *In:* ORGANIZATION, U. N. I. D. (ed.) *6th IIR International Conference on Sustainability and the Cold Chain.* Nantes, France.

WANG, C., CHENG, C., JIN, T. & DONG, H. 2022. Water evaporation inspired biomass-based PCM from daisy stem and paraffin for building temperature regulation. *Renewable Energy,* 194, 211-219.

WANG, K., HU, C., CAI, Y., LI, Y. & TANG, D. 2023. Investigation of heat transfer and flow characteristics in two-phase loop thermosyphon by visualization experiments and CFD simulations. *International Journal of Heat and Mass Transfer,* 203, 123812.

YE, C., ZHENG, M. G., WANG, M. L., ZHANG, R. H. & XIONG, Z. Q. 2013. The design and simulation of a new spent fuel pool passive cooling system. *Annals of Nuclear Energy,* 58, 124-131.

ZHANG, H., SHI, Z., LIU, K., SHAO, S., JIN, T. & TIAN, C. 2017. Experimental and numerical investigation on a CO2 loop thermosyphon for free cooling of data centers. *Applied Thermal Engineering,* 111, 1083-1090.

ZHANG, P., WANG, B., SHI, W., HAN, L. & LI, X. 2015. Modeling and performance analysis of a two-phase thermosyphon loop with partially/fully liquid-filled downcomer. *International Journal of Refrigeration,* 58**,** 172-185.